Catalysis Science & Technology

Accepted Manuscript

This article can be cited before page numbers have been issued, to do this please use: A. Erigoni, G. Paul, M. Meazza, M. C. Hernandez-Soto, I. Miletto, R. Rios, C. Segarra, L. Marchese, R. Raja, F. Rey, E. Gianotti and U. M. Diaz, *Catal. Sci. Technol.*, 2019, DOI: 10.1039/C9CY01609K.

ROYAL SOCIETY OF CHEMISTRY

rsc.li/catalysis

View Article Online
DOI: 10.1039/C9CY01609K

ARTICLE

Acid Properties of Organosiliceous Hybrid Materials Based on Pendant (Fluoro)Aryl-Sulfonic Groups through Spectroscopic Study with Probe Molecules

Received 00th January 20xx,
Accepted 00th January 20xx

DOI: 10.1039/x0xx00000x

Andrea Erigoni,[a] Geo Paul,[b] Marta Meazza,[c] María Consuelo Hernández-Soto,[a] Ivana Miletto,[b] Ramón Ríos,[c] Candela Segarra,[a] Leonardo Marchese,[b] Robert Raja,[c] Fernando Rey,[a] Enrica Gianotti*[b] and Urbano Díaz *[a]

Two different heterogeneous catalysts carrying aryl-sulfonic moieties, in which the aromatic ring was either fluorinated or not, were successfully synthetized. The multi-step synthetic approaches implemented involved the synthesis of the silyl-derivative, template-free one-pot co-condensation (at low temperature and neutral pH) and tethering reaction. A multi-technique approach was implemented to characterize the hybrid organic-inorganic catalysts involving TGA, N_2 physisorption analysis, FTIR, ss MAS NMR (^{1}H, ^{13}C, ^{29}Si). Specifically, the acidity of the organosiliceous hybrid materials was studied through the adsorption of probe molecules (i.e. CO at 77 K and NH_3 and TMPO at room temperature) and a combination of FTIR and ss MAS NMR spectroscopies. The catalytic activity of the two hybrids was tested in the acetal formation reaction between benzaldehyde and ethylene glycol. Preliminary results indicated superior performances for the fluoro-aryl-sulfonic acid, compared to the non-fluorinated sample. The findings hereby reported opens up to the design of heterogeneous sulfonic acids with superior reactivity in acid catalyzed reactions. Moreover, through the implementation of spectroscopic studies, using probe molecules, it was possible to investigate in detail the acidic properties of hybrid organosiliceous materials.

Introduction

Since the early days of heterogeneous catalysis, scientists have tried to mimic nature in designing catalysts with ever higher conversion and selectivity. Hybrid materials, formed by the combination of inorganic and organic building units, are attractive for the purpose of creating high-performance or highly functionalized structures[1–3]. Combining the advantages of inorganic solids (high mechanical, thermal, and structural stability) and organic molecules or macromolecules (flexibility and functionality), they are suitable for a wide range of applications, including catalysis[4], adsorption[5], separations[6], microelectronics[7], photoluminescence[8]. Organosilica based materials are by far the most used support to develop type II[9] hybrid catalysts[2], due to the simplicity of their synthesis, their tuneable textural properties and the highly reactive surface, which makes them the ideal platform support for grafting or tethering additional active sites[10]. Among the different approaches to incorporate organic moieties into inorganic frameworks[2], sol-gel chemistry and in particular the co-condensation of a mixture of siloxanes together with organo-silanes is one of the most commonly used[11–13]. Interestingly, one-pot synthesis methods of several hybrid organic-inorganic materials by a fluoride-catalysed synthesis have been described in the state-of-art[12]. This strategy offers numerous advantages such as low synthesis temperatures, nearly neutral pH and absence of templating agents, at the same time providing final porous materials with high surface area and tuneable porosity[14]. The purely siliceous solids obtained present high surface area (up to 1000 m^2/g) and a non-ordered system of mesopores (so called NOS-type materials). These properties, together with a highly reactive surface, make them the ideal platform systems for developing novel supported hybrid organic-inorganic catalysts. In order to covalently bond the organic molecule with the silica framework, the former needs to be functionalized with an alkoxy-silyl group that will eventually undergo hydrolysis/condensation, together with the silica precursors[15–17].

Sulfonic acids are one of the many functional groups that have been used to prepare silica based heterogeneous organocatalysts baring strong acid sites[18] for carrying out esterification of fatty acids[19], acetalization reactions[20], acetal hydrolysis[21]. The effect of nearby atoms on the catalytic

[a] Instituto de Tecnología Química, Universitat Politècnica de València-Consejo Superior de Investigaciones Científicas, Avenida de los Naranjos s/n, E-46022 Valencia, Spain. E-mail: udiaz@itq.upv.es
[b] Department of Science and Technological Innovation, Universitá del Piemonte Orientale, Viale T. Michel 11, 15121 Alessandria, Italy. E-mail: enrica.gianotti@uniupo.it
[c] School of Chemistry, University of Southampton, Highfield Campus, SO17 1BJ, Southampton, UK

Electronic Supplementary Information (ESI) available: ^{1}H and ^{13}C NMR spectra of silyl derivative compounds. FTIR difference spectra in the OH and CO stretching region of CO adsorption at 80 K on HSO_3-NOS-H and HSO_3-NOS-F hybrid materials.

activity of sulfonic acids has been studied and industrially exploited for several decades. For example, propyl- and aryl-sulfonic acids were supported onto amorphous silica and their activity was compared in the reaction of anisol with acetic anhydride[22], showing a beneficial effect of having the sulfonic group bounded to an aromatic ring. An even more representative example of the effect of the chemical makeup of the sulfonic acid on its catalytic activity are fluorinated alkylsulfonic acids[23–26]. The inductive effect provided by having fluorine as a substituent on the carbon in α position greatly enhance the acidity of the proton. Nevertheless, the synergistic effect of having the sulfonic group bounded onto a fluorinated aromatic ring has not deeply been explored taking into account the interaction of acid active groups with the silica surface. In this work, we report the synthesis of supported aryl-sulfonic acid organocatalysts onto NOS-type materials. To investigate the inductive effect of fluorine on the aryl-sulfonic groups and, ultimately, on its acidity two different catalysts were designed and compared. In one of them the aromatic ring was fluorinated in the other was not. The two hybrid materials underwent a deep physic-chemical characterization aimed to study morphology, textural properties, thermal stability and spectroscopic properties. Specifically, a combination of FTIR and multinuclear solid state NMR methods were implemented. Additionally, probe molecules of different basic strength were adsorbed/desorbed onto the hybrids. Gaseous or highly volatile bases such as carbon monoxide, ammonia, pyridine and pyridine derivatives have been widely used as probe molecules to study the acidic properties of purely inorganic catalysts[27–29]. Nevertheless, within the field of organosiliceous hybrid catalysts, this insightful characterization approach remains unexplored. In this study, for the first time, carbon monoxide and ammonia were adsorbed on the surface of the hybrids and their interaction was followed both by FTIR and ss NMR in order to assess the acidity of the hybrid catalysts. The results obtained from this characterization study was decisive to better explain the catalytic activity in solid-acid catalysed reactions.

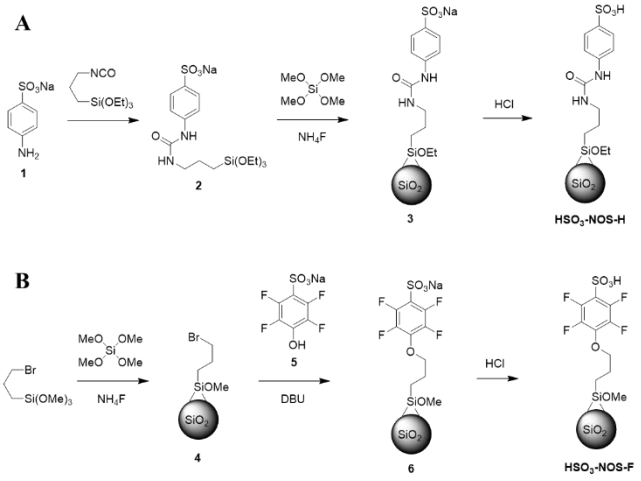

Scheme 1: Representation of the synthesis of the supported sulfonic acids

Results and Discussion

To modulate the acid strength in sulfonic hybrid catalysts, two different organic moieties containing protonated or fluorinated aryl-sulfonic acid groups were developed. The synthesis of the two hybrid catalysts containing aryl-sulfonic groups, was carried out following two different approaches (Scheme 1). In the case of hybrid with protonated aromatic ring named **HSO_3-NOS-H** (A), sulfanilic acid was firstly reacted with NaOH to achieve its sodium form (**1**) and enhance its solubility in acetonitrile. The silyl derivative carrying the sodium sulfonate group (compound **2**) was obtained through the reaction of the primary amine present on the phenyl ring of **1** with 3-(triethoxysilyl)propyl isocyanate (acetonitrile, 65 °C, N_2), which led to the formation of the urea group as indicates the liquid (^{1}H and ^{13}C) NMR spectra (Fig. S1 and S2). The peaks observed were consistent with the desired product, specifically the ^{13}C signal centred at 160 ppm is typical of the carbonyl carbon in the urea group. The synthesis of the heterogeneous catalyst was obtained by co-condensation of **2** and tetramethyl orthosilicate (TMOS), carried out in methanol and water (1:1). Hydrolysis and condensation of the alkoxy groups was catalysed by F^- ions, which acted as mineralizing agents[12].

As mentioned above, this approach presents several advantages, as the synthesis was carried out at 36 °C, for 24 h, under mild pH conditions, using low amounts of solvent and catalyst. Moreover, the textural properties (specific surface area and mean pore size) could be tuned by varying the F^- concentration and the chain length of the alcohol used as co-solvent[12]. The synthesis of hybrid with fluorinated aromatic ring named **HSO_3-NOS-F** (B) underwent a slightly different approach (Scheme 1). Substrate **5** resulted insoluble in any solvent besides H_2O and DMSO. Implementing the former would have been detrimental for the alkoxy groups of the silyl-derivative. Using the latter would have required very high temperature for its distillation. Such high temperature might have promoted the spontaneous condensation of the alkoxy groups of the organosilane compounds and their partial polymerization. To avoid this problem, a Br-propyl functionalized NOS was first synthetized. Afterwards, the solid was reacted with **5**, previously mixed with DBU (1,8-diazabicyclo[5.4.0]undec-7-ene) to promote the deprotonation of the hydroxyl group, leading to a non-porous hybrid material with pendant (fluoro)aryl-sulfonic groups (**6**).

In both synthetic pathways, the exchange of sodium with a proton was achieved by suspending 3 and 6 in an HCl solution in EtOH. The total exchange of Na was checked by ICP analysis. **HSO_3-NOS-H** and **HSO_3-NOS-F** underwent a deep physico-chemical characterization. Firstly, thermogravimetric analysis was recorded on both samples to measure the organic content and to probe the thermal stability of the materials. The weight losses (TGA) and their respective DTA curves of the materials are reported in Fig. 1. The first weight loss undergone by both materials occurs between 70 and 150 °C and it's associated

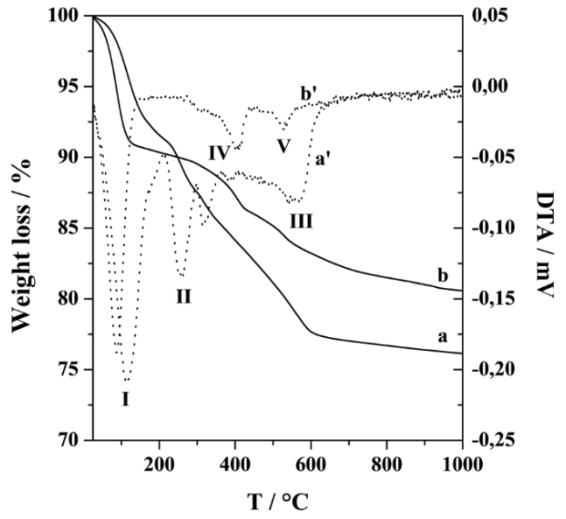

Figure 1: TGA and DTA curves of HSO_3-NOS-H (a, a') and HSO_3-NOS-F (b, b').

with the removal of physisorbed water (I). Focusing on HSO_3-NOS-H (curves a, a'), a second weight loss is observed between 250-380 °C (II). This is probably due to the breakage of the urea bond and consequent desorption of the phenyl-sulfonic moieties[21]. Finally, a loss between 500-600 °C is due to the decomposition of the propyl chain anchored to the surface (III). Considering this as the limit temperature for the total decomposition of the organic moieties supported onto the silica, the loss resulted to be about 15% of the overall weight (temperature range between 200 and 600 °C). Shifting to HSO_3-NOS-F (curves b, b'), after the initial loss due to the desorption of physisorbed water, a main weight loss due to the organic moieties is observed at about 300-450 °C and it is related to the breakage of the ether bond linking the fluorinated phenyl ring to the propyl chain (IV). Lastly, a weight loss between 500 and 600 °C was bestowed to the thermal decomposition of the alkyl chains, still anchored onto the silica surface (V). The total weight loss due to the organic moieties

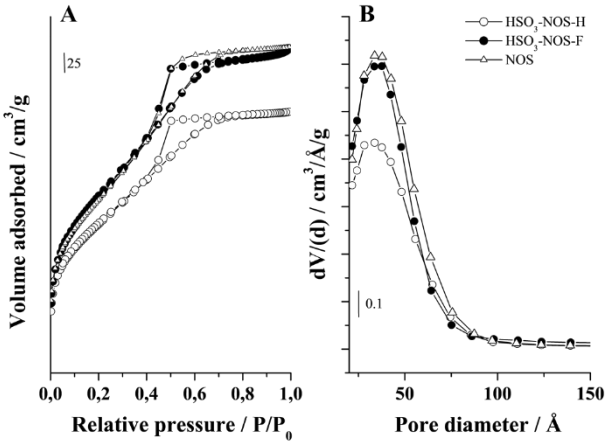

Figure 2: A) N_2 adsorption/desorption isotherms at 77 K of HSO_3-NOS-H, HSO_3-NOS-F and non-ordered silica (NOS, reference material). B) Pore-size distribution of the materials in the mesopores range.

was about 8.4% of the total weight. In both hybrid solids, a progressive weight loss at temperatures above 600 °C was detected due to dehydroxylation phenomena, i.e. condensation of external silanol groups with the release of water molecules and formation of strained siloxane bridges. The TGA results evidenced that probably the thermal stability of the ether groups is slightly higher than the urea groups, being HSO_3-NOS-F sample more stable than HSO_3-NOS-H, from a thermal point of view. After investigating the amount and the stability of the organic species constituting the hybrid materials, the focus was shifted to the textural properties. N_2 physisorption analysis at 77 K was recorded on the two hybrid catalysts and on a pure silica sample obtained with the same synthetic methodology in order to study the specific surface area and the free porous volume of the materials and the effect of the presence of the R-Si(OR')$_3$ species in the synthesis mixture (Figure 2, Table 1). The isotherms show a type IV behaviour (IUPAC), with a hysteresis loop typical of conventional mesoporous materials. The N_2 uptake is also compatible with mesoporous materials obtained through F^- catalysed sol-gel approach. Furthermore, cavitation and bottle-ink pore shape could give hysteresis and sharp jump in the desorption band[12]. The Brunauer-Emmet-Teller (BET) method was used to obtain information regarding the surface area of the catalysts. Both organo-catalysts shows a surface area comparable with the one of the pure silica reference material (802 m^2/g). Specifically, HSO_3-NOS-F provides an area of 816 m^2/g whereas HSO_3-NOS-H shows a surface area of 683 m^2/g. This slightly lower value may be related to the usage of a bulkier organosilane precursor used in the one-pot synthesis of the solid. The adsorption branches of the isotherms were analysed by means of (i) NLDFT (non-localized density functional theory) and (ii) Barrett-Joyner-Halenda (BJH) methods to obtain information on the pore-size distributions. Both functionalized non-ordered silicas and the reference pure silica material show a pore distribution spacing between 20 and 60 Å with a peak centred at about 35 Å, typical for non-ordered silica materials obtained through F^- sol-gel synthesis process[12]. In all three samples a small amount of micropores is present. This was already observed in other synthesis carried out in NH_4F medium[12,21]. After exploring the amount and the stability of the organic moieties and the textural properties of the hybrid catalysts, a ss NMR and FTIR spectroscopic characterization was carried out to study the organic-inorganic interaction and to assess the acidic properties of the hybrids[30]. Prior recording the FTIR spectra, all the samples have been outgassed at 453 K for 2 h in order to remove physisorbed water. HSO_3-NOS-H spectrum (Fig.3, curve c) appears quite different compared with the pure silica reference material, NOS (Fig.3, curve a). The presence of the bulky silyl-derivative in the synthesis leads to a lower amount of isolated silanols in the final material: a signal centred at 3745 cm^{-1}, due to the O-H stretching mode of Si-OH groups, is visible but its intensity is much lower than the reference material. Instead, a broad signal related to silanols interacting with each other through H-bond is visible between 3500-3200 cm^{-1}. A number of signals related to stretching mode of C-H

View Article Online
DOI: 10.1039/C9CY01609K

Table 1: Textural properties of HSO_3-NOS-H and HSO_3-NOS-F. Microporous and mesoporous contribution to surface area and pore volume were estimated by means of non-linear DFT method. VBJH was calculated from the adsorption branch of the isotherms.

	SSA_{BET} m^2/g	SSA_{DFT} m^2/g	SA_{Micro} m^2/g	SA_{meso} m^2/g	V_{BJH} cm^3/g	V_{DFT} cm^3/g	V_{micro} cm^3/g	V_{meso} cm^3/g
HSO_3-NOS-H	683	549	91	458	0.39	0.485	0.0301	0.455
HSO_3-NOS-F	816	613	36	577	0.49	0.6	0.0163	0.584
NOS	802	607	80	527	0.52	0.643	0.027	0.616

groups present in the aromatic ring, in the propyl linker and in eventual uncondensed alkoxy groups are visible between 3000-2800 cm^{-1}. The low frequencies region appears quite rich in signals, due to the presence of the urea group. A signal centred at at 1685 cm^{-1} is attributed to the stretching modes of the C=O bond of the urea group. The presence of the urea group is confirmed by the amide II band, centred at 1600 cm^{-1}, which is related to a motion combining N-H bending and C-N stretching of the amide group[31]. Lastly a sharp band at 1535 cm^{-1} is bestowed to the C-C stretching of the aromatic ring. In addition, a weak band at 1380 cm^{-1} is visible due to the S=O asymmetric stretching mode of sulfonic groups. Shifting the focus on HSO_3-NOS-F FTIR spectrum (Fig.3, curve b), it can be observed that by using a less bulky silyl-derivative as organosilane precursor, the amount of isolated silanols (3745 cm^{-1}) in the resulting materials appears comparable to the pure silica one. A composed signal centred between 3000-2800 cm^{-1} is observed and bestowed to the stretching mode of C-H groups present in the propyl chains (and in uncondensed alkoxy groups). Due to the simpler liking point between the propyl chain and the aryl-sulfonic moieties, in this spectrum, the low frequency region appears poorer in signals, with a sharp band centred at 1500 cm^{-1}, related to the C-C stretching of the fluorinated aromatic ring. In order to study the acidity of the sulfonic groups exposed to the inorganic silica surface, CO was adsorbed at 80 K on the hybrid catalysts (Fig. S3). Both materials behave equally upon interaction with CO. Focusing on the high frequency region, the signal related to the stretching modes of isolated silanols (3745 cm^{-1}) is shifted downward, forming a broad signal centred at approximately 3644 cm^{-1}. The 100 cm^{-1} frequency shift is coherent with previous studies reported on purely siliceous materials[28]. In the CO stretching region, at low coverages a signal centred at 2155 cm^{-1} arose, due to the CO molecules in interaction with the SiOH groups on the surface of the support[28]. At higher CO dosages the typical band related to the stretching mode of the free CO molecule appears (ν_{CO} liquid-like at 2138 cm^{-1})[32]. Given a specific site with which the CO is interacting, the blue shift of its the stretching mode is expected to be proportional to the ability of the site to accept electronic density, i.e. its acidity.

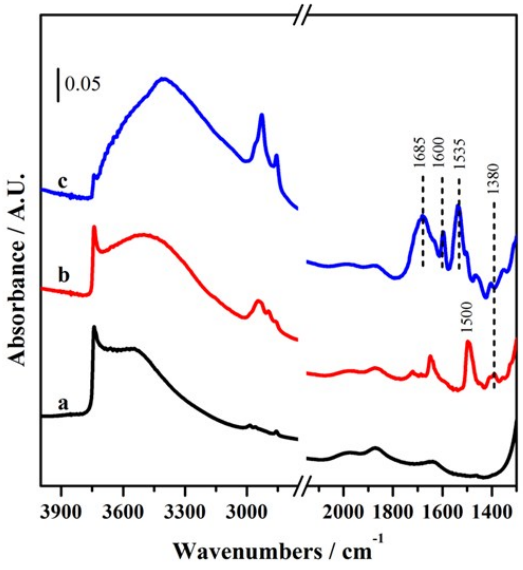

Figure 3: FTIR spectra of non-ordered silica (NOS, curve a), HSO3-NOS-F (curve b) and HSO3-NOS-H (curve c). The samples have been outgassed at 453 K prior recording the spectra.

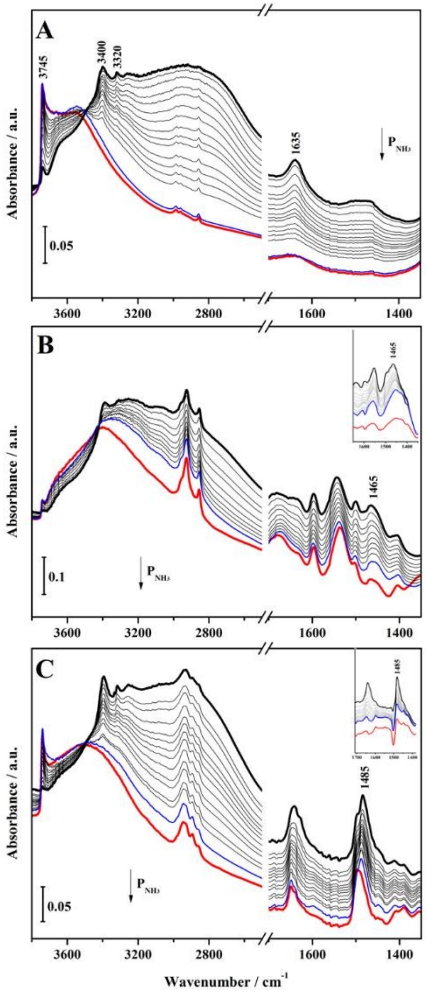

Figure 4: FTIR spectra of NH_3 adsorption at 298 K on NOS (A), HSO_3-NOS-H (B), HSO_3-NOS-F (C). Red curves: hybrids in vacuum before NH_3 adsorption, Black curves: adsorption of high NH_3 pressure (30 mbar), Blue curves: NH_3 outgassing at rt. B and C insets: FTIR difference spectra

Nevertheless, despite the presence of highly acidic sulfonic groups, no signal is observed at higher frequencies than that of CO interacting with silanols. The CO adsorption at 80 K is able to reveal only the mild acidity due to the available Si-OH of the inorganic support. The high concentration of external silanol groups masks the presence of sulfonic groups present in the hybrid materials. Then, a more selective probe molecule has been used, such as ammonia. NH_3 was adsorbed at room temperature on the hybrids and on pure non-ordered silica support (Fig.4). NH_3 interaction with NOS (Fig.4A), produced the typical features due to the formation of H-bond between Si-OH groups of the silica and the probe molecule[33]. At high NH_3 pressure (30 mbar), bands at 3400 and 3320 cm^{-1} appear, overlapped to a broader band centred at 3020 cm^{-1} while the band at 3745 cm^{-1}, due to the O–H stretching mode of free silanols (red curve), almost completely disappears (bold black curve). The broad band centred at 3020 cm^{-1} is assigned to the O–H stretching of the silanol groups H-bonded to NH_3 molecules. The bands at 3400 and 3320 cm^{-1} are respectively due to the N-H asymmetric and symmetric stretching modes of NH_3 bonded to silanols. At lower frequency, a bands at 1635 cm^{-1} is also present assigned to the asymmetric bending mode of the ammonia molecules adsorbed on Si–OH groups. Such complexes are very weakly held as demonstrated by the fact that all their spectroscopic features progressively fade away when decreasing the NH_3 pressure and almost completely disappear upon outgassing the sample at room temperature for 30 minutes (blue curve), giving a spectrum which is similar to that of the bare NOS sample before NH_3 adsorption (red curve). Differently from the behaviour observed upon NH_3 adsorption of pure silica mesoporous support, the ammonia adsorption on both HSO_3-NOS-H (Fig.4B) and HSO_3-NOS-F (Fig.4C) hybrids produced, in the low frequency region, the bands at 1465 and 1485 cm^{-1} due to the asymmetric bending mode of NH_4^+ protonated species, meaning that sulfonic acid groups are strong enough to protonate ammonia[34]. The ammonia protonation is irreversibly process, in fact upon NH_3 desorption at room temperature, the signal due to NH_4^+ ions is still visible on both hybrid catalysts (blue curves). In the insets are reported the difference FTIR spectra in order to better evidence the formation of the NH_4^+ bands that are partially overlapped to other signals typical of the organic part of the hybrids.

A suite of multi-nuclear magic angle spinning nuclear magnetic resonance (MAS NMR) spectroscopic experiments has been used to study the hybrid organic-inorganic mesoporous silica based catalysts. The successful incorporation of aryl-sulfonic acids on non-ordered mesoporous silica was established by ^{29}Si NMR spectroscopy while the integrity of the organic components on the hybrid catalyst was determined by ^{13}C NMR spectroscopy. This information gave a first idea on local arrangements of organosilane species and furthermore supported by various ^1H MAS NMR methods which would help to determine the proton environments as well as the acidic nature of the catalysts. ^{29}Si population distribution as well as the organosilane functionalization in different hybrid catalysts was studied by ^{29}Si CPMAS NMR. Fig. 5 (left panel) shows the ^{29}Si CPMAS NMR spectra of hybrid catalysts, where both Q and T Si sites are present[30]. There are three different Q silicon sites, namely Q^4 ($Si(OSi)_4$) silicon sites (at around -110 ppm), Q^3 ($Si(OSi)_3OH$) silicon sites (at around -100 ppm) and Q^2 ($Si(OSi)_2(OH)_2$) silicon sites (at around -90 ppm) seen in hybrid catalysts originating from the non-ordered mesoporous silica support. On the other hand, signals from T^3 ($RSi(OSi)_3$) silicon sites (at around -66 ppm) and T^2 ($RSi(OSi)_2OH$) silicon sites (at around -58 ppm) stem from the organosilane groups confirm their successful silica surface functionalization[21]. Similarly, Fig. 5 (right panel) shows the ^{13}C CPMAS NMR spectra of as synthesized hybrid catalysts. The assignments of the spectral resonances are based on either ^{13}C solution-state NMR or on software predicted computed spectra. In fact, the ^{13}C CPMAS NMR spectra of the hybrid catalysts presents the typical ^{13}C signals associated with organosilane groups confirming the integrity of the synthesis process. On the other hand, the incomplete hydrolysis of alkoxy groups from the precursors is clearly evident through the presence of their peaks (at around 15, 50 and 59 ppm). The weak aromatic resonances (110 to 145 ppm) in HSO_3-NOS-F catalyst are due to the fact that no protons are directly attached to the phenyl carbons as the intensity of ^{13}C resonances depends on the proton-carbon dipolar interactions in a CPMAS experiment. In addition, presence of unreacted 3-bromopropyl silane was also detected in this sample. ^1H MAS and spin-echo NMR spectra of hybrid catalysts, previously treated at 180 °C for 90 minutes in vacuum, recorded at a MAS rate of 15 kHz are shown in Fig. 6, left and right panel, respectively. Firstly, the intense resonance at 1.7 ppm is attributed to isolated silanols originating from the mesoporous silica support and the broad shoulder in the range 2-10 ppm to hydrogen bonded silanols[35]. However, contributions from water, amine protons and sulfonic acid protons also fall in this broad shoulder as they are in mutually exchangeable state. Exchangeable protons undergo different binding dynamics and forms spatially structured clusters of

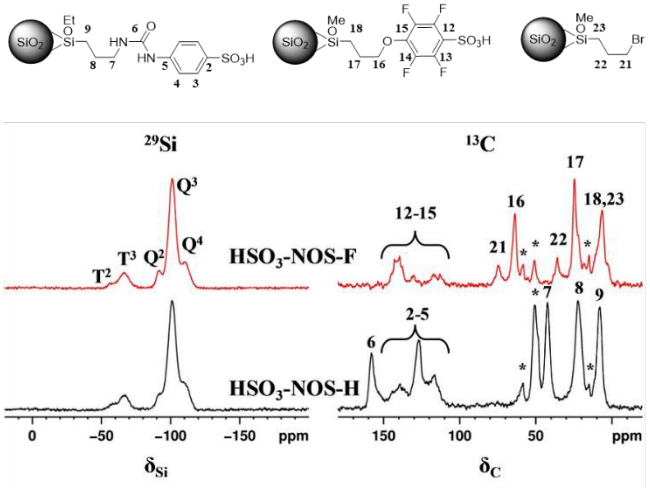

Figure 5: ^{29}Si (left panel) and ^{13}C (right panel) CPMAS NMR spectra of various hybrid catalysts recorded at 10 kHz MAS rate. A CP contact time of 2ms was employed for ^{29}Si CPMAS while for ^{13}C CPMAS a value of 4ms and 20ms were used for samples HSO_3-NOS-H (red *curves) and HSO_3-NOS*-F (black curves), respectively.

View Article Online
DOI: 10.1039/C9CY01609K

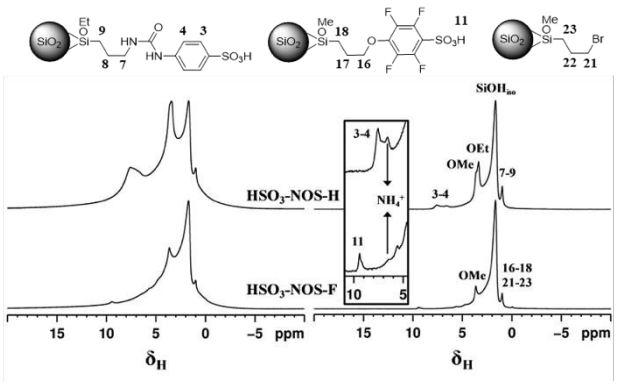

Figure 6: ^{1}H MAS (left panel) and 1H spin-echo (right panel) NMR spectra of various hybrid catalysts recorded at 15 kHz MAS rate. An echo delay (tau) of 2ms was used in the spin-echo experiment. Inset shows the zoomed spectra.

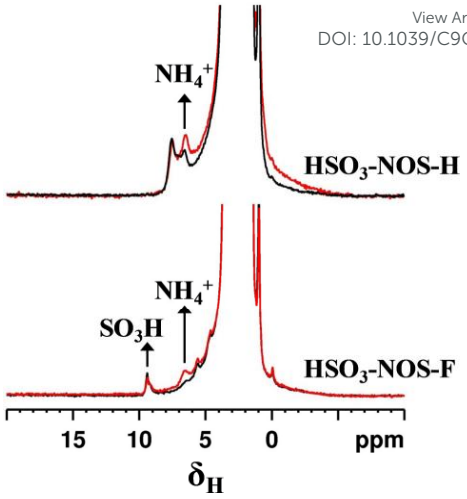

Figure 7: ^{1}H spin-echo NMR spectra of various hybrid catalysts, before (black) and after (red) ammonia adsorption, recorded at 15 kHz MAS rate and an echo delay (tau) of 2ms.

variable sizes with chemical shift values determined by exchange between bound water, free water, isolated SiOH, hydrogen bonded SiOH and acidic/basic protons. The resulting ^{1}H chemical shift is the weighted shift of the compounds which are involved in the fast chemical exchange[36]. Furthermore, proton resonance peaks associated with organosilanes are clearly detected at around 1 ppm for aliphatic components and at around 7.5 ppm for aromatic units. No aromatic protons were detected in HSO_3-NOS-F catalyst as they are substituted by fluorine. Sharp resonance peaks in the range 3.2 to 3.6 are attributed to alkoxy groups from the unhydrolysed precursors. It is important to note that peaks due to residual ammonium fluoride, used as a catalyst in the synthesis of non-ordered mesoporous silica, were detected at 6.6 ppm. Finally, the narrow low intensity resonance detected at 9.4 ppm in HSO_3-NOS-F catalyst is attributed to sulfonic acid protons (Fig. 6, inset) not in exchange with other compounds. Acidity of the hybrid catalysts were determined by adsorbing a basic probe molecule that would be converted to protonated species upon contact with acidic sulfonic protons. Ammonia was adsorbed on the hybrid catalysts that were previously treated at 180°C in vacuum for 90 minutes. ^{1}H spin-echo NMR spectra were recorded after ammonia adsorption and are shown in Fig. 7. It is clearly evident that ammonium ions were formed after adsorption as the intensity of 6.6 ppm peak has increased. Furthermore, a small decrease in the peak intensity of sulfonic acid protons is also observed in sample HSO_3-NOS-F. It is important to note that every single sulfonic acid proton would be converted into four equivalent ammonium ion protons upon adsorption. Presence of a 9.4 ppm peak in the spectrum after ammonia adsorption also confirms the fact that not all sulfonic acid protons are accessible to ammonia. On the other hand, marked increase in the formation of ammonium ions in sample HSO_3-NOS-H after ammonia adsorption is surprising as no free sulfonic acid protons were detected in ^{1}H NMR spectrum of parent sample. As has been pointed out earlier, the sulfonic acid protons are in exchangeable state (either with water or with silanols or both) in this sample, however, can easily protonate a stronger base upon its presence. On the other hand, sulfonic acid proton signals can also be overlapped with other signals or the resonance can be broadened due to stronger dipolar interactions. In order to

circumvent such issues, we have employed a different probe molecule to determine the acid strength on these hybrids. It is well established that ^{31}P MAS NMR chemical shift scale can be used to determine the acidic strength of solid acids by adsorbing trimethylphosphine oxide (TMPO)[30]. The larger the ^{31}P NMR down-field shift of adsorbed TMPO molecule, the higher is the acidity of the material[37,38]. Fig. 8A shows the room temperature ^{31}P MAS NMR spectra of HSO_3-NOS-H and HSO_3-NOS-F after the TMPO adsorption. Both samples exhibit an intense peak at 47 ppm, assigned to physisorbed TMPO molecules. Interestingly, resonance peaks at 89 and 90 ppm in HSO_3-NOS-H and HSO_3-NOS-F, respectively, confirms the very strong acidity displayed by these hybrids. A recent article has charted the acid strength of super acids using ^{31}P MAS NMR spectroscopy and the largest chemical shift for TMPO was reported to be 93 ppm for a sulfonated polymer embedded in montmorillonite[39]. Therefore, it can be concluded that the aryl-sulfonic acid based catalysts presented in this work display acid strength similar to 100% H_2SO_4 (Fig. 8B) The higher ^{31}P MAS NMR chemical shift for catalyst HSO_3-NOS-F confirms the higher acidity of this hybrid catalyst. To summarize, solid-state NMR methods delivered detailed information on the local structure of organosilanes and dynamics of sulfonic protons. The presence of acidity of the catalysts were evidenced, by protonation of ammonia upon adsorption, through a ^{1}H peak at 6.6 ppm as well as by TMPO adsorption and ^{31}P peak observation at around 90 ppm. Moreover, the structural integrity of the organosilane units as well as the hybrid nature of the silica backbone were confirmed by ^{13}C and ^{29}Si CPMAS NMR experiments, respectively. The solid-acid catalysts outlined in Scheme 1 (HSO_3-NOS-H and HSO_3-NOS-F) were evaluated in the acetal formation reaction between benzaldehyde and ethylene glycol as shown in Scheme 2. This reaction is of particular interest to synthetic organic chemists, as it is used to protect aldehydes and ketones, making them stable under basic reaction conditions, to facilitate subsequent reduction and oxidation transformations[41,42]. Preliminary catalytic findings as outlined in Figure 9, show promising catalytic trends, in both reactivity and recyclability, demonstrating the potential of these type of heterogeneous catalysts. The anchored catalyst HSO_3-NOS-F demonstrates a slightly higher stability, showing high quantitative yields and recyclability under the experimental reaction conditions, thereby vindicating the robustness of the anchoring strategy for creating hybrid heterogeneous catalysts. Catalyst HSO_3-NOS-H shows a slightly lower activity, under the same reaction conditions, probably due to its lower acidity. It is highly likely that the presence of fluorine atoms in the benzene ring of catalyst HSO_3-NOS-F makes it more electron-poor, inducing a higher degree of acidity in the sulfonic acid moiety, compared to the urea derivative present in catalyst HSO_3-NOS-H.

We also investigated the scope of the acetalization reaction with different aldehydes and ketones with catalyst HSO_3-NOS-

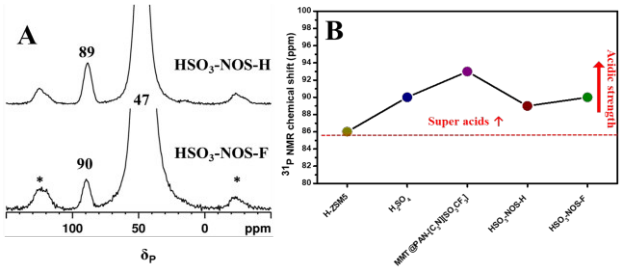

Figure 8: ^{31}P MAS NMR spectra (A) of various hybrid catalysts recorded at room temperature and a MAS rate of 15 kHz. * denote spinning sidebands. A graph (B) showing the acid strength versus ^{31}P MAS NMR chemical shifts of various super acids catalysts reported in the literature (see reference 39).

Table 2: Evaluating the wider scope of anchored catalyst, HSO_3-NOS-H, for acetalization and trans-acetalization reactions

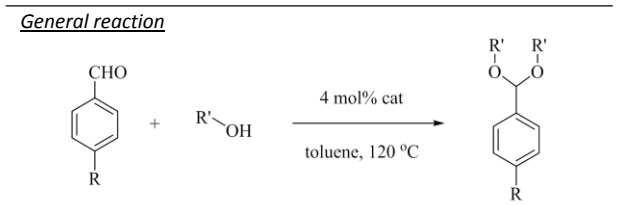

Aldehyde/ketone	Alcohol	Yield %
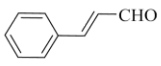	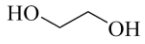	56
R = NO_2	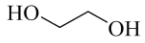	100
R = OMe	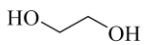	10
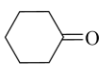	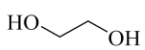	100
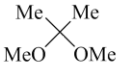	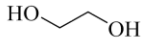	60
R = NO_2	CH_3OH	16

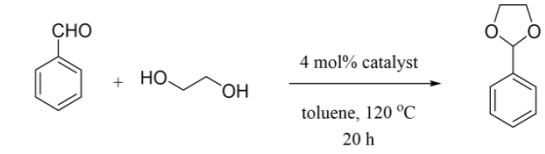

Scheme 2: Catalytic reaction used to test the reactivity and recyclability of HSO_3-NOS-H and HSO_3-NOS-F catalysts

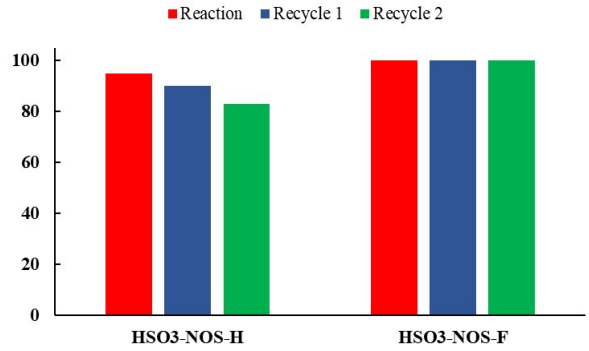

Figure 9: Yields obtained with HSO_3-NOS-H and HSO_3-NOS-F catalysts in the acetalization reaction.

H to evaluate the wider potential of these anchored catalysts containing pendant acid sites (Table 2). Promising results were obtained when cyclohexanone and other electron-poor benzaldehydes were employed as substrates. As expected, electron-rich aldehydes represent a challenge due to their electronic nature and require longer reaction times or harsher reaction conditions. To evaluate wider industrial applicability, we also probed the effectiveness of these anchored catalysts in the trans-acetalization reaction achieving promising results when dimethoxy propane was used (60% yield).

Experimental

Synthesis of the materials

Synthesis of 2. Compound **1** was achieved by reacting sulfanilic acid (99%, Aldrich) with 1 equivalent of NaOH, in H_2O. **1** was reacted with 3-(triethoxysilyl)propyl isocyanate (95%, Aldrich) in acetonitrile, at 65 °C, under N_2, overnight. The solvent was then evaporated under vacuum.

Synthesis of 3. A solution of **2**, tetramethyl orthosilicate (98%, Aldrich), MeOH and H_2O was prepared and stirred until complete dissolution (solution A). A solution of NH_4F (Aldrich, 98%) in H_2O was prepared (solution B). Solution B was added to solution A and stirred at room temperature until gelation occurred. The gel obtained was aged at 36 °C for 24 h. Afterwards, the solid was dried overnight at 65 °C, grinded and washed with ethanol and H_2O. The final composition of the synthesis gel was the following: 0.97TMOS : 0.03RSi(OR')$_3$: 4MeOH : 4H_2O : 0.00313NH_4F.

Synthesis of 4. The material was obtained using the same procedure as the synthesis of 3, using (3-bromopropyl)trimethoxysilane (97%, Fluorochem) instead of using compound **2**.

Synthesis of 6. A solution of **5** (Sodium 2,3,5,6-tetrafluoro-4-hydroxybenzenesulfonate, 98%, TCI Europe) in DMSO was prepared under N_2. DBU(1,8-Diazabicyclo[5.4.0]undec-7-ene, 97.5%, Aldrich) was added and the mixture was stirred for 10 minutes. Br-propyl functionalized silica (**4**) was added and the mixture was stirred at 100 °C for 16 h. Afterwards the suspension was cooled down at room temperature and the solid was filtered and washed abundantly with H_2O and ethanol.

Synthesis of HSO_3-NOS-H and HSO_3-NOS-F. The supported sodium sulfonates **3** and **6** were exchanged three times with a 0.05 M HCl solution in EtOH at room temperature.

Catalytic test

The anchored, solid-acid catalysts, **HSO_3-NOS-H and HSO_3-NOS-F** (4 mol%) were added into a glass-lined reactor, equipped with a Dean Stark apparatus and a condenser, followed by subsequent addition of the aldehyde (1 equiv, 0.5 mmol), dialcohol (30 equiv) and toluene (5 ml). The reaction was stirred at 120 °C for 20 h and the yield was quantified by ^{1}H-NMR using an internal standard. Recycling: The crude reaction was filtered, the catalyst was washed with dichloromethane, dried under vacuum and reused in the next reaction.

Characterization

^{1}H and ^{13}C NMR spectra were recorded on a Bruker 300 spectrometer and the chemical shifts are reported in ppm relative to residual proton solvent signals. Nitrogen adsorption isotherms were measured at 77 K with a Micromeritics ASAP 2010 volumetric adsorption analyser. Before the measurement, the sample was outgassed for 12 hours at 80 °C. The BET specific surface area was calculated from the nitrogen adsorption data in the relative pressure range from 0.04 to 0.2. The total pore volume was obtained from the amount of N_2 adsorbed at a relative pressure of about 0.99. The pore diameter and the pore size distribution were obtained using the Barrett– Joyner–Halenda (BJH) method on the adsorption branch of the isotherms. The adsorption branch of the N_2 physisorption isotherm was analysed by means of the NLDFT (nonlocal density functional theory) method, to obtain the pore size distribution of the materials. Thermogravimetric analyses (TGA/DTA) of materials were performed under argon flow (100 mL min^{-1}) with a SETSYS Evolution TGA-DTA/DSC thermobalance, heating from 40 to 1000 ºC at 5 ºC min^{-1}. FTIR spectra of self-supporting pellets were collected under vacuum conditions (residual pressure <10^{-5} mbar) using a Bruker Equinox 55 spectrometer equipped with a pyroelectric detector (DTGS type) with a resolution of 4 cm^{-1}. CO was adsorbed at 77K and NH_3 was adsorbed at room temperature using specially designed cells permanently connected to a vacuum line to perform adsorption–desorption *in situ* measurements. FTIR spectra were normalized with respect the pellet weight and, whenever specified, are reported in difference-mode by subtracting the spectrum of the sample in vacuum from the spectrum of the adsorbed molecules. Solid-state NMR spectra were acquired on a Bruker Advance III 500 spectrometer and a wide bore 11.7 Tesla magnet with operational frequencies for ^{1}H, ^{13}C, ^{31}P and ^{29}Si of 500.13, 125.77, 202.47 and 99.35 MHz, respectively. A 4 mm triple resonance probe with MAS was employed in all the experiments. The samples were packed on a Zirconia rotor and spun at a MAS rate between 10 and 15 kHz. The magnitude of radio frequency (RF) fields were 100 and 42 kHz for ^{1}H and ^{29}Si, respectively. The relaxation delay between accumulations was 2 and 2.5 s. For the ^{13}C and ^{29}Si Cross Polarization (CP) MAS experiments, the RF fields of 55 and 28 kHz were used for initial proton excitation and decoupling, respectively. During the CP period the ^{1}H RF field was ramped using 100 increments, whereas the ^{13}C/^{29}Si RF fields were maintained at a constant level. During the acquisition, the protons are decoupled from the carbons/silicons by using a two-pulse phase-modulated (TPPM) decoupling scheme. A moderate ramped RF field of 62 kHz was used for spin locking, while the carbon/silicon RF field was matched to obtain optimal signal. A rotor-synchronised spin-echo sequence

View Article Online
DOI: 10.1039/C9CY01600K

(π/2--τ--π--τ--acquisition) was also applied to record the ^{1}H NMR spectra with delay time τ of 2 ms. The delay time was chosen as an optimised compromise between the signal decay owing to relaxation and the resolution gain owing to longer delay times. ^{31}P MAS NMR spectra were recorded using high power proton decoupling and the RF field for the 90 degree pulse were 83 kHz. All chemical shifts are reported using δ scale and are externally referenced to tetramethylsilane (TMS) at 0 ppm for ^{1}H, ^{13}C and ^{29}Si. Ammonium dihydrogenphosphate (1 ppm) was used as standard for the ^{31}P nucleus.

Prior to the adsorption of TMPO probe molecules, the catalysts were packed onto a 4 mm zirconia rotor and evacuated at 180 °C for 90 minutes in high vacuum line. After that, TMPO dissolved in anhydrous dichloromethane was added to the rotor and rapidly closed with a cap and left for adsorption for one hour. Later, the rotor was opened and attached back to the high vacuum line for the complete removal of dichloromethane at room temperature. Subsequently, the rotor was closed with a zirconia cap and heated to 160 °C for 30 minutes followed by submission to NMR spectral recording.

Conclusions

In this work, two novel organosiliceous hybrid catalysts containing sulfonic acids were successfully synthetized through a multi-step approach. One of them, namely HSO_3-NOS-H contains aryl-sulfonic groups; while the other, HSO_3-NOS-F, has aryl-sulfonic groups in which the aromatic ring is fluorinated. The textural properties of the materials showed characteristics typical of mesoporous materials, with a BET surface area of about 600-700 m^2/g and a narrow pore size distribution centred at about 35 Å, which is particularly notable considering that the co-condensation of the TMOS and the silyl-derivatives was carried out in absence of templating agents. Moreover, the successful incorporation of organic functionalities opens up to the possibility of designing porous catalysts for specific substrates of different size and functionalities, as by simply changing gel composition, textural properties (specifically, pore size) can be tuned[7,12]. FTIR spectroscopy, together with ^{1}H, ^{13}C and ^{29}Si solid state MAS NMR were implemented to study the integrity of the organic moieties and the speciation of the silicon atoms within the hybrid materials. The adsorption of a strong base such as ammonia as probe molecule followed by FTIR and ^{1}H spin-echo NMR has allowed to study the acidic behaviour of the two type of sulfonic acids, highlighting that the hybrid with fluorinated aryl-sulfonic groups has a greater availability of the acid sites. On the other hand, ^{31}P MAS NMR data on the TMPO adsorbed hybrid catalysts revealed the super acidic nature of the materials. Preliminary catalytic results indicate the superior performance and recyclability of HSO_3-NOS-F catalyst, compared to the HSO_3-NOS-H analogue, highlighting the effectiveness of the anchoring strategy. The acidic nature of the organosiliceous hybrids can be suitably modulated to influence the catalytic properties of the materials and the wider potential of these anchored catalysts in trans-acetalization reactions affords scope for their industrial applicability. By capitalizing on the structure-property links, derived from the design methodology and associated characterization, we can devise catalytic applications that vindicate the merits of solid-acid centres on hybrid heterogeneous catalysts.

Conflicts of interest

There are no conflicts to declare.

Acknowledgements

AE acknowledge “la Caixa” foundation for PhD scholarship. The authors are grateful for financial support from the European Union by the MULTY2HYCAT EU-Horizon 2020 funded project under grant agreement no. 720783.

Notes and references

1 A. Corma, U. Díaz, T. García, G. Sastre and A. Velty, *JACS*, 2000, 132, 15011.
2 U. Díaz, D. Brunel and A. Corma, *Chem. Soc. Rev*., 2013, 42, 4083.
3 C. Sanchez, B. Julián, P. Belleville and M. Popall, *J. Mater. Chem.*, 2005, 15, 3559.
4 M. P. Kapoor, A. K. Sinha, S. Seelan, S. Inagaki, S. Tsubota, H. Yoshida and M. Harutad, *Chem. Comm.*, 2002, 23, 2902.
5 D. J. Collins and H. Zhou, *J. Mater. Chem.*, 2007, 17, 3154.
6 Ö. Dag, C. Yoshina-Ishii, T. Asefa, M. J. MacLachlan, H. Grondey, N. Coombs and G. A. Ozin, *Adv. Funct. Mater.*, 2001, 11, 213.
7 K. J. Shea and D. A. Loy, *Chem. Mater.*, 2001, 13, 3306.
8 B. V. Harbuzaru, A. Corma, F. Rey, P. Atienzar, J. L. Jordá, H. García, D. Ananias, L. D. Carlos, J. Rocha, *Angew. Chemie Int. Ed.*, 2008, 47, 1080.
9 C. Sanchez and F. Ribot., *New J. Chem.,* 1994, 18, 1007.
10 F. Hoffmann, M. Cornelius, J. Morell and M. Fröba, *Angew. Chemie Int. Ed*., 2006, 45, 3216.
11 A. Stein, B. J. Melde and R. C. Schroden, *Adv. Mater*., 2000, 12, 1403.
12 E. Reale, A. Leyva, A. Corma, C. Martinez, H. Garcia and F. Rey, *J. Mater. Chem.,* 2005, 15, 1742.
13 M. H. Lim, C. F. Blanford and A. Stein, *JACS*, 1997, 119, 4090.
14 R. Winter, D. W. Hua, P. Thiyagarajan and J. Jonas, *J. Non. Cryst. Solids*, 1989, 108, 137.
15 S. Llopis, T. García, A. Cantín, A. Velty, U. Díaz and A. Corma. *Catal. Sci. Technol*., 2018, 8, 5835.
16 B. P. Pichon, M. Wong Chi Man, P. Dieudonné, J.-L. Bantignies, C. Bied, J.-L. Sauvajol and J. J. E. Moreau, *Adv. Funct. Mater.*, 2007, 17, 2349.
17 C. González-Arellano, A. Corma, M. Iglesias and F. Sánchez, *Adv. Synth. Catal.,* 2004, 346, 1316.
18 E. Doustkhah, J. Lin, S. Rostamnia, C. Len, R. Luque, X. Luo, Y. Bando, K. C.-W.Wu, J. Kim, Y. Yamauchi and Y. Ide, *Chem. A Eur. J*., 2018, 25, 1614.
19 I. K. Mbaraka, B. H. Shanks, *J. Catal.*, 2005, 229, 365.
20 W.-J. Zhou, L. Fang, Z. Fan, B. Albela, L. Bonneviot, F. De Campo, M. Pera-Titus and J.-M. Clacens, *JACS*, 2014, 136, 4869.
21 E. Gianotti, U. Diaz, A. Velty, and A, Corma, *Catal. Sci. Technol.*, 2013, 3, 2677.

View Article Online
DOI: 10.1039/C9CY01609K

22 C. G. Piscopo, G. Maestri, E. Paris, V. Santacroce and R. Maggi, *Arkivoc*, 2015, 1.
23 A. G. Posternak, R. Y. Garlyauskayte and L. M. Yagupolskii, *Tetrahedron Lett.*, 2009. 50, 446.
24 G. A. Olah, M. Arvanaghi and V. V. Krishnamurthy, V. V., *J. Org. Chem*., 1983, 48, 3359.
25 G. A. Olah, K. Laali and A. K. Mehrotra, *J. Org. Chem.*, 1983, 48, 3360.
26 J. N. Armor, *Appl. Catal. A Gen*., 2001, 222, 407.
27 I. Miletto, G. Paul, S. Chapman, G. Gatti, L. Marchese, R. Raja and E. Gianotti, *Chem. A Eur. J.*, 2017, 23, 9952.
28 A. Erigoni, S. H. Newland, G. Paul, L. Marchese, R. Raja and E. Gianotti, *ChemCatChem*, 2016, 8, 3161.
29 S. Bordiga, P. Ugliengo, A. Damin, C. Lamberti, G. Spoto, A. Zecchina, G. Spanò, R. Buzzoni, L. Dalloro, F. Rivetti., *Top. Catal.,* 2001, 15, 43.
30 C. A. Trickett, T. M. Osborn Popp, J. Su, C. Yan, J. Weisberg, A. Huq, P. Urban, J. Jiang, M. J. Kalmutzki, Q. Liu, J. Baek, M. P. Head-Gordon, G. A. Somorjai, J. A. Reimer and O. M. Yaghi, *Nat. Chem.,* 2019, 11, 170-176.
31 G. Socrates, *Infrared and Raman characteristic group frequencies: tables and charts,* Wiley, Chichester, 3rd edn, repr. as paperback., 2010
32 M. S Holm, S. Svelle, F. Joensen, P. Beato, C. H. Christensen, S. Bordiga and M. Bjorgen, *Appl. Catal. A Gen*., 2009, 356, 23.
33 E. Gianotti, V. Dellarocca, L. Marchese, G. Martra, S. Coluccia and T. Maschmeyer, *Phys. Chem. Chem. Phys.,* 2002, 4, 6109.
34 A. Zecchina, L. Marchese, S. Bordiga, C. Pazè and E. Gianotti, *J. Phys. Chem. B*, 1997, 101, 10128.
35 G. Paul, G. Musso, E. Bottinelli, M. Cossi, L. Marchese and G. Berlier, *ChemPhysChem*, 2017, 18, 839–849..
36 M. Sharifi, M. Wark, D. Freude and J. Haase, *Microporous Mesoporous Mater.*, 2012, 156, 80.
37 A. Zheng, S. Li, S.-B. Liu and F. Deng, *Acc. Chem. Res*., 2016, 49, 655.
38 A. Zheng, S.-B. Liu and F. Deng, *Solid State Nucl. Magn. Reson.*, 2013, 55–56, 12.
39 F. Liu, X. Yi, W. Chen, Z. Liu, W. Chen, Chen-Ze Qi, Yu-Fei Song and A. Zheng, *Chem. Sci.,* 2019, 10, 5875-5883 (see references included here).
40 A. Zheng, S. B. Liu and F. Deng, *Chem. Rev*., 2017, 117, 12475-12531.
41 P. G. Wuts and T. W. Greene, *Greene's protective groups in organic synthesis*, Wiley, 2006.
42 H. Firouzabadi, N. Iranpoor and B. Karimi, *Synlett*, 1999, 321.

Hybrid heterogeneous catalysts containing (fluoro)aryl-sulfonic groups were characterizedthrough combined spectroscopic techniques and adsorption of probe molecules, being modulated their reactivity for acetals formation.